

## Electrochemical Oxidation of Cyanide Using Platinized Ti Electrodes

Aušra VALIŪNIENĖ<sup>1\*</sup>, Vaidas ANTANAVIČIUS<sup>1</sup>, Žana MARGARIAN<sup>1</sup>,  
Ieva MATULAITIENĖ<sup>2</sup>, Gintaras VALINČIUS<sup>3</sup>

<sup>1</sup> Department of Physical Chemistry, Vilnius University, Naugarduko 24, LT-03225 Vilnius, Lithuania

<sup>2</sup> Center for Physical Sciences and Technology, Savanorių ave. 231, LT-02300 Vilnius, Lithuania

<sup>3</sup> Vilnius Gediminas Technical University, Saulėtekio al. 11, LT-10223 Vilnius, Lithuania

**crossref** <http://dx.doi.org/10.5755/j01.ms.19.4.2514>

Received 26 September 2012; accepted 10 March 2013

The cyanide-containing effluents are dangerous ecological hazards and must be treated before discharging into the environment. Anodic oxidation is one of the best ways to degrade cyanides. Pt anodes as the most efficient material for the cyanide electrochemical degradation are widely used. However, these electrodes are too expensive for industrial purposes. In this work Ti electrodes covered with nano-sized Pt particle layer were prepared and used for the anodic oxidation of cyanide ions. Surface images of Ti electrodes and Ti electrodes covered with different thickness layer of Pt were compared and characterized by the atomic force microscopy (AFM). The products formed in the solution during the CN<sup>-</sup> ions electrooxidation were examined by the Raman spectroscopy. An electrochemical Fast Fourier transformation (FFT) impedance spectroscopy was used to estimate the parameters that reflect real surface roughness of Pt-modified Ti electrodes.

*Keywords:* platinized titanium, electrooxidation, cyanide.

### 1. INTRODUCTION

Cyanide may be found in a wide variety of organic and inorganic compounds as a carbon-nitrogen radical. In some forms it acts as a very powerful and fast toxin. Cyanide can enter surface water through releases from metal finishing industries, iron and steel mills, runoff from disposal of cyanide wastes in landfills, pesticides, and the use of cyanide containing road salts [1]. The cyanide-containing effluents are dangerous ecological hazards and must be treated before discharging into the environment. Therefore, based on toxicity tests, many regulatory agencies are imposing strict regulations with regard to a point – source cyanide emission limits [2].

One of the most commonly applied methods for the destruction of cyanide involves oxidation of cyanide waste by air oxygen in large lagoons [3]. However, storage of such toxic substances, especially in big amounts, poses great risks to humans and the environment, and may trigger legal liability in case of accidental spill. Typical methods for the destruction of cyanides involve chemical and/or electrochemical oxidation. Chemical methods require special substances and sludge disposal. Effective alternatives to typical chemical oxidation treatments are the methods of electrochemical oxidation [4–6]. These methods are advantageous because there is no need of additional chemicals. In addition, during the electrolysis, heavy metals present in cyanide electrolytes may be collected on a cathode, consequently, both the destruction of cyanides and the removal of heavy metals can be accomplished simultaneously [7, 8].

Electrochemical methods of cyanide oxidation have been studied by many authors since 1970's [9–16]. However, the challenge to find cheap and simple method for the high-yield cyanide oxidation still remains topical.

Thus, aiming at developing ecologically friendly and economically reasonable processes for decontamination of cyanide, we investigated Ti anode surfaces coated with layers of Pt nanoparticles, which, we believe, could be an attractive alternative to expensive Pt anodes. The objectives of present work are: (i) to analyze and compare Ti electrodes of varying thickness of Pt coatings using surface imaging by AFM; (ii) to determine the products formed in the solution during the CN<sup>-</sup> ion electrooxidation by Raman spectroscopy; (iii) to analyze the electrochemical impedance spectra of electrochemical oxidation of cyanide, and to determine parameters that characterize surface roughness of investigated electrodes.

### 2. EXPERIMENTAL DETAILS

All solutions were prepared using distilled water. Cyanide electrooxidation was carried out in 0.1 molL<sup>-1</sup> of KCN (puriss. p. a. “Fluka”) solution. The surface area of the working electrodes (Ti, and different platinized Ti) was 2 cm<sup>2</sup>. Working electrode was mechanically polished, degreased and rinsed with distilled water before each experiment. Two stainless steel plates were used as counter electrodes. All experiments were performed at 20 °C temperature.

Ti electrodes were covered by different amount of Pt, which is equivalent of a theoretical, 100 % yield, metal thickness equal to 200 nm, 500 nm and 1000 nm. These thicknesses are used throughout the paper as parameters to distinguish between different types of tested electrodes, however, real surface coverage was dependent on current yields, which typically varied from 40 % to 60 %, and morphology of electrodeposits. Electrodeposition was carried out in the electrolyte containing 3.764 gL<sup>-1</sup> Pt

(puriss p. a. “Alfa Aesar GmbH & Co”, Germany) and  $250 \text{ g L}^{-1}$  HCl (puriss p. a., “Standard”, Poland). The applied current density was  $1.5 \text{ mA cm}^{-2}$  and time of electrolysis was calculated according to thickness of Pt. Before electrochemical platinization Ti (99.2 % pure, “Alfa Aesar GmbH & Co”, Germany) plate was polished with the diamond paste and then washed in the ultrasonic baths.

Veeco (USA) measuring system “Catalyst”, in which the atomic force microscope is connected with the optical microscope “Olympus IX71”, was used to analyze the changes in the surface roughness of the Pt covered Ti electrodes (varying in thickness), and the active surface area in each. The optical microscope was used as a tool to help choose and verify the correct reading position of the atomic microscope. Aiming to measure as accurately as possible the surface of the target electrode, experiments were performed using the contact setting. The images were collected and viewed using an atomic force microscope software “Gwyddion 2.10”.

Raman Spectroscopy was used to monitor the change in  $\text{CN}^-$  ion concentration in solution as the electrochemical oxidation occurred. Raman spectra were recorded by RamanFlex 400 (PerkinElmer, Inc.) spectrometer with a thermoelectrically cooled detector. Each spectrum was collected with integration time of 10 s and accumulation of 30 scans, yielding total acquisition time 300 s.

All electrochemical impedance spectra were recorded under the potentiostatic setting, using FFT impedance spectrometer EIS-128/16. The reference electrode was a saturated Ag/AgCl, KCl electrode, placed as close as possible to the working electrode by means of a Luggin capillary.

### 3. RESULTS AND DISCUSSION

Surface images of different platinum – coated Ti (0, 200, 500 and 1000 nm) electrodes were obtained using an atomic force microscope. The results were analyzed using the computer program “Gwyddion 2.10”, with which surface roughness root mean square (RMS), the surface area, and the relative size of the particles were determined. Figure 1 shows surface images of polished Ti (a) and Pt covered Ti: 200 nm (b), 500 nm (c) and 1000 nm (d). The RMS of polished Ti electrode surface was found to be 308 nm RMS (Table 1). Upon deposition of 200 nm Pt layer, spherical Pt crystal formation is observed (Figure 1 (b)), while the measured electrode surface RMS increased to 369 nm. 500 nm Pt layer, indicated an RMS of 469 nm, while 1000 nm layer indicated noticeable decrease of RMS to 356 nm (Table 1). Meanwhile, the real surface area follows similar pattern. It increases up to 500 nm, while 1000 nm Pt layers shows slight decrease, which, we believe, reflect overlap of growing spheroids of electrodeposited Pt, as it is evident from Figure 1 (d).

The average size of the Pt particles on the Ti electrode covered by 200 nm and 500 nm Pt layers varies from  $0.5 \mu\text{m}$  to  $2.0 \mu\text{m}$  (Figure 1 (a), (b), and Table 1). Their density follows Pt thickness increase and reaches maximum in 1000 nm (Figure 1 (d)) layers of Pt.

Particle size variation is non - monotonic. It increases from 200 nm to 500 nm, and then starts decreasing as the

Pt thickness reach 1000 nm (Figure 1 and Table 1). The data in Figure 1 and Table 1 show that the RMS parameter has a direct correlation with the active surface area. That is, surface roughness increases proportionally to the active surface area.

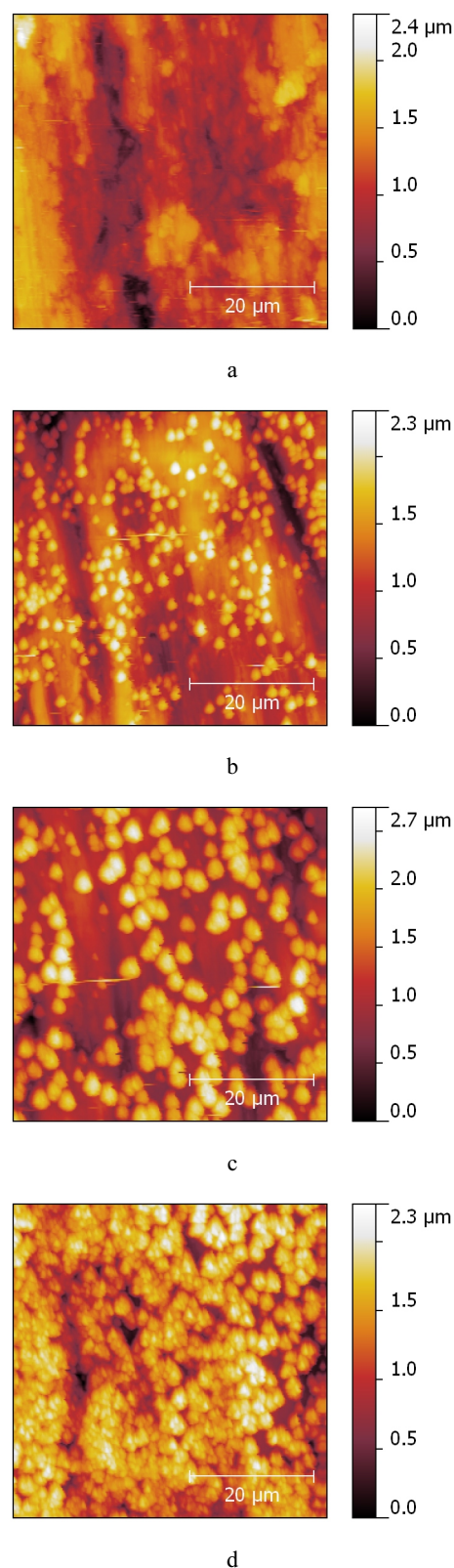


**Fig. 1.** AFM images of electrode surface: (a) polished Ti surface, (b), (c), (d) same Ti surface covered with different layer of Pt. (b) – 200 nm; (c) – 500 nm; (d) – 1000 nm

**Table 1.** Parameters of the investigated electrodes obtained by AFM

Electrodes	Real surface area, m <sup>2</sup>	RMS, nm	The size of Pt particles, μm
Ti (pure)	2.6×10 <sup>-9</sup>	308	–
Ti + 200 nm Pt	2.8×10 <sup>-9</sup>	369	0.5–0.8
Ti + 500 nm Pt	3.0×10 <sup>-9</sup>	469	1–2
Ti + 1000 nm Pt	2.9×10 <sup>-9</sup>	356	0.5–2

It was determined [17] that Ti electrodes covered with a thicker than 400 nm Pt layer are suitable for the electrochemical oxidation of cyanides. Therefore, aiming to analyze the content of the products formed in the cyanide solution during the process of electrochemical oxidation, the 1000 nm Pt-coated Ti electrode was chosen.

It is not entirely clear which products that are formed during the KCN electrochemical oxidation: CO<sub>3</sub><sup>-</sup>, NH<sub>4</sub><sup>+</sup> or CON<sup>-</sup> is final [9, 18]. To clarify this situation Raman measurements were performed (Fig. 2). During the electrochemical oxidation recorded Raman spectra show decrease of the primary product (2080 cm<sup>-1</sup> band) and the appearance of reaction products – two bands at 1067 cm<sup>-1</sup> and 1048 cm<sup>-1</sup>, as well as the intermediate product at 2170 cm<sup>-1</sup>.

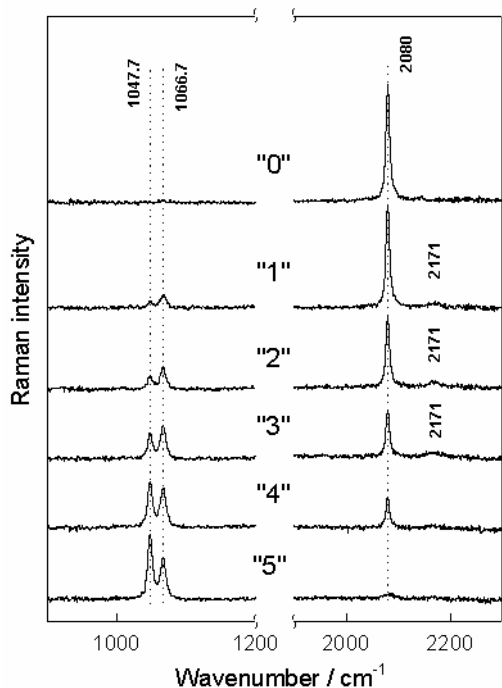


**Fig. 2.** Raman spectra of KCN solutions. "0" solution before electrochemical oxidation, "1–5" solutions after each hour of reaction

Our data suggest that during the reaction three different products are formed. For the purpose of assigning these shifts we performed Raman measurements of the possible products (Fig. 3). From the additional measurements we have determined that the CON<sup>-</sup> is indeed the intermediate product (at 2170 cm<sup>-1</sup>). One of the possible final products could be CO<sub>3</sub><sup>2-</sup>, where 1063 cm<sup>-1</sup> is the symmetric stretching vibrational mode of anion [19,20]. However we were unable to specify the other final product of the reaction, we would need to perform additional experiments and do quantum chemical calculations.

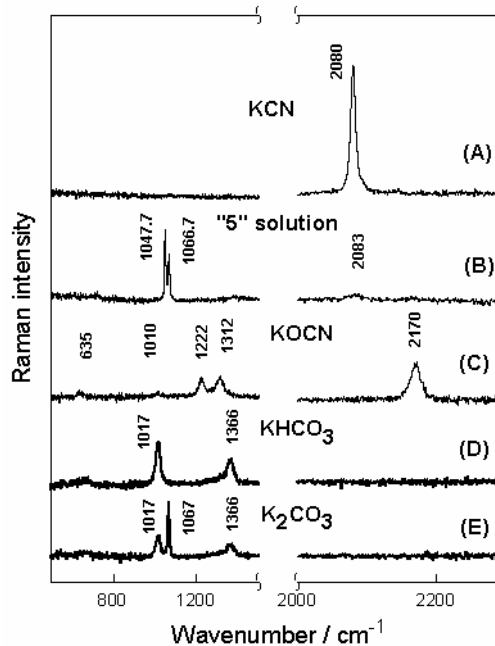


**Fig. 3.** Additional Raman spectra. Primary solution of KCN (A), final product (B), possible final products: KOCN (C), KHCO<sub>3</sub> (D) and K<sub>2</sub>CO<sub>3</sub> (E)

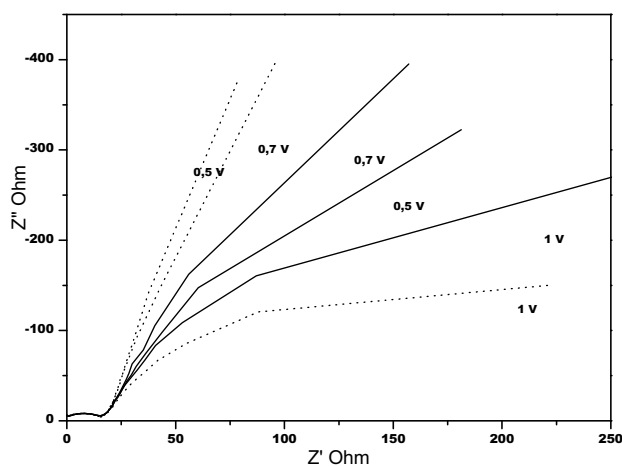


**Fig. 4.** Electrochemical FFT impedance spectra. Solution composition: 0.1 M KCN. (–) before electrolysis and (···) after electrolysis. Used electrode: Ti + 500 nm Pt

From the voltammetric measurements it was determined [17] that electrochemical oxidation of cyanide occurs simultaneously with water electrolysis process, when electrode potential exceeds 1.1 V. Under lower voltage conditions, the Faraday process practically does not occur. In this study, the electrochemical impedance spectra of Ti and Pt covered Ti surfaces were recorded, at bias potentials 0.5 V, 0.7 V and 1.0 V. The electrochemical impedance spectra obtained using Ti electrode covered with 500 nm Pt layer are presented in Figure 4. The spectra obtained using Ti, and Ti covered with 200 nm and 1000 nm Pt layer are not provided. Before the analysis of the EIS spectra, the validation of measured impedance data by comparing the spectra of perturbation voltage and response current was tested [21]. It was checked how the measured frequencies of response correspond to frequencies of perturbing signal.

It was determined that in the range of frequencies over 1000 Hz, there are numerous additional frequencies in impedance spectrum, whose origin we were not able to determine. Therefore for the EIS data analysis such frequencies were rejected. We chose an electrochemical equivalent circuit taking into account the fact that in our system the Faraday process occurs (Fig. 5).

**Table 2.** The values of equivalent circuit (Fig. 5) obtained by analyzing FFT electrochemical impedance spectra of cyanide electrooxidation

Ti (pure) electrode before electrolysis			
	0.5 V	0.7 V	1.0 V
$R_0, \Omega$	13.22	13.31	12.7
$CPE, F$	$6.45 \times 10^{-5}$	$5.7 \times 10^{-5}$	$5.2 \times 10^{-5}$
$n$	0.876	0.887	0.88
$R_{ct}, \Omega$	–	–	–
Ti + 200 nm Pt electrode before electrolysis			
	0.5 V	0.7 V	1.0 V
$R_0, \Omega$	12.09	12.03	11.87
$CPE, F$	$1.72 \times 10^{-4}$	$1.57 \times 10^{-4}$	$1.5 \times 10^{-4}$
$n$	0.894	0.898	0.89
$R_{ct}, \Omega$	3686	5329	1756
Ti + 500 nm Pt electrode before electrolysis			
	0.5 V	0.7 V	1.0 V
$R_0, \Omega$	14.61	14.95	14.44
$CPE, F$	$4.81 \times 10^{-4}$	$4.18 \times 10^{-4}$	$4.46 \times 10^{-4}$
$n$	0.783	0.805	0.77
$R_{ct}, \Omega$	–	–	–
Ti + 1000 nm Pt electrode before electrolysis			
	0.5 V	0.7 V	1.0 V
$R_0, \Omega$	16.7	17.18	12.54
$CPE, F$	$5.23 \times 10^{-4}$	$4.29 \times 10^{-4}$	$4.96 \times 10^{-4}$
$n$	0.78	0.812	0.787
$R_{ct}, \Omega$	–	–	–
Ti + 200 nm Pt electrode after electrolysis			
	0.5 V	0.7 V	1.0 V
$R_0, \Omega$	13.1	13.31	13.38
$CPE, F$	$5.46 \times 10^{-5}$	$4.78 \times 10^{-5}$	$4.1 \times 10^{-5}$
$n$	0.87	0.88	0.89
$R_{ct}, \Omega$	8289	12547	5796
Ti + 500 nm Pt electrode after electrolysis			
	0.5 V	0.7 V	1.0 V
$R_0, \Omega$	15.57	15.64	14.99
$CPE, F$	$4.2 \times 10^{-4}$	$4.06 \times 10^{-4}$	$5.17 \times 10^{-4}$
$n$	0.848	0.845	0.78
$R_{ct}, \Omega$	–	–	1021
Ti + 1000 nm Pt electrode after electrolysis			
	0.5 V	0.7 V	1.0 V
$R_0, \Omega$	14.28	14.09	12.95
$CPE, F$	$4.36 \times 10^{-4}$	$4.359 \times 10^{-4}$	$6.63 \times 10^{-4}$
$n$	0.797	0.79	0.7
$R_{ct}, \Omega$	–	–	–

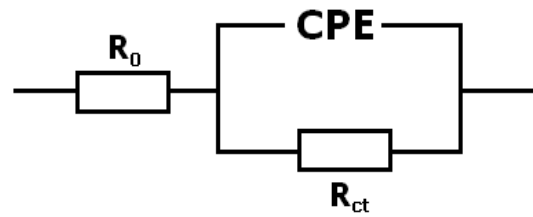


**Fig. 5.** Equivalent circuit.  $R_0$  – the uncompensated solution resistance,  $R_{ct}$  – the charge transfer resistance,  $CPE$  – the constant phase element

In this case, the equivalent circuit consists of three elements: solution resistance  $R_0$ , constant phase element  $CPE$ , which represents the electric double layer (EDL) which forms at the electrode-solution interface, and parallel resistance  $R_{ct}$  that represents the charge transfer.

Using EIS data analysis software “Zview” we obtained satisfactory fit of the experimental data to the model equivalent circuit. The fit parameters are presented in Table 2.

Analyzing the parameters in the Table 2, it is obvious that  $CPE$  is minimal for the pure Ti electrode. The  $CPE$  values increase as the thickness of the Pt layer on the Ti electrode increases. This can be associated with the increasing surface area in the process of platinization of Ti.

The obtained  $CPE$  values may not be compared with capacitance of double electric layer because the exponential degree  $n$  is too far from 1. This shows that the electrochemical process on all investigated electrodes is limited not solely by the EDL charging-discharging, but also by other simultaneously occurring processes. Parallel resistance of  $R_{ct}$  contributes to measured EIS only in the case of the Ti electrode covered by 200 nm Pt layer. In other cases,  $R_{ct}$  influence is negligible. This effect requires further investigation.

Over all, EIS data correlate well with the results obtained by AFM, and show that both the real surface area and capacitance of EDL of platinized Ti electrodes increase with the thickness of Pt layer.

#### 4. CONCLUSIONS

The surface morphology and electrical parameters of Ti and platinized Ti electrodes was characterized by AFM and EIS. Covering Ti surface with layers of Pt causes RMS of the electrodes to increase from ~308 nm (pure Ti) to ~369 nm (Ti+200 nm Pt) and up to 469 nm (Ti+500 nm Pt). We found that the size of the deposited Pt spheroids varies in a non-monotonic way reaching maximum at 500 nm. An overlap of spheroids was observed at 1000 nm Pt films, while the average size of Pt particles started decreasing at this thickness. AFM results correlated well with the EIS data. Generally, we claim that EIS may be used to monitor the development of Pt coating morphology and real surface area.

Using Raman spectroscopy we detected three products of electrochemical oxidation. One of them is an intermediate  $CNO^-$ , and the other is the final product  $CO_3^{2-}$ . The third product was not identified. To do this we will need further measurements and possibly theoretical calculations.

## Acknowledgments

This work was supported by the Lithuanian ESF agency grant (code VP1-3.1-ŠMM-08-K-01-014).

## REFERENCES

1. **Dash, R. R., Gaur, A., Balomajumder, C.** Cyanide in Industrial Wastewaters and Its Removal: A Review on Biotreatment *Journal of Hazardous Materials* 163 2009: pp. 1–11.
2. **Hofseth, C. S., Chapman, T. W.** Electrochemical Destruction of Dilute Cyanide by Copper-catalyzed Oxidation in a Flow-through Porous Electrode *Journal of the Electrochemical Society* 146 (1) 1999: pp. 199–207.
3. **Marsden, J., House, I.** The Chemistry of Gold Extraction. Ellis Harwood, London, 1992.
4. **Ho, S. P., Wang, Y. Y., Wan, C. C.** Electrolytic Decomposition of Cyanide Effluent with an Electrochemical Reactor Packed with Stainless-steel Fiber *Water Research* 24 1990: pp. 1317–1321.
5. **Bergman, H., Hertwig, H., Nieber, F.** Experimental and Theoretical-studies on a New Type of Electrochemical Reactor for Waste-water Treatment *Chemical Engineering Processing* 31 1992: pp. 195–203.
6. **Buso, A., Giomo, M., Boaretto, L., Sandona, G., Paratella, A.** New Electrochemical Reactor for Wastewater Treatment: Electrochemical Characterization *Chemical Engineering Processing* 36 1997: pp. 255–260.
7. **Szpyrkowicz, L., Kaul, S. N., Molga, E., DeFavery, M.** Comparison of the Performance of a Reactor Equipped with a Ti/Pt and SS Anode for Simultaneous Cyanide Removal and Copper Recovery *Electrochimica Acta* 46 (2–3) 2000: pp. 381–387.
8. **Szpyrkowicz, L., Zilio-Grandi, F., Kaul, S. N., Polcaro, A. M.** Copper Electrodeposition and Oxidation of Complex Cyanide from Wastewater in an Electrochemical Reactor with a Ti/Pt Anode *Industrial & Engineering Chemistry Research* 39 2000: pp. 2132–2139.
9. **Arikado, T., Iwakura, C., Yoneyama, H., Tamura, H.** Anodic Oxidation of Potassium Cyanide on Graphite Electrode *Electrochimica Acta* 21 1976: pp. 1021–1027.
10. **Hine, F., Yasuda, M., Iida, T., Ogata, Y.** On the Oxidation of Cyanide Solutions with Lead Dioxide Coated Anode *Electrochimica Acta* 31 1986: pp. 1389–1395.
11. **Arellano, C. A. P., Martinez, S. S.** Indirect Electrochemical Oxidation of Cyanide by Hydrogen Peroxide Generated at a Carbon Cathode *International Journal of Hydrogen Energy* 32 (15) 2007: pp. 3163–3169.
12. **Osathaphan, K., Chucherdwatanasak, B., Rachdawong, P., Sharma, V. K.** Effect of Ethylenediaminetetraacetate on the Oxidation of Cyanide in an Electrochemical Process *Journal of Environmental Science and Health A* 43 (3) 2008: pp. 295–299.
13. **Pedraza-Avella, J. A., Acevedo-Pena, P., Pedraza-Rosas, J. E.** Photocatalytic Oxidation of Cyanide on TiO<sub>2</sub> *An Electrochemical Approach. Catal. Today* 133 2008: pp. 611–618.  
<http://dx.doi.org/10.1016/j.cattod.2007.12.063>
14. **Su, Y., Li, Q., Wang, Y., Wang, H., Hong, J.** Silver Recovery and Cyanide Removal from Silver-plating Wastewater Using Pulse-electrolysis *Huagong Xuebao/CIESC J.* 60 (9) 2009: pp. 2308–2313.
15. **Yeddou, A. R., Nadjemi, B., Halet, F., Ould-Dris, A., Capart, R.** Removal of Cyanide in Aqueous Solution by Oxidation with Hydrogen Peroxide in Presence of Activated Carbon Prepared from Olive Stones *Minerals Engineering* 23 (1) 2010: pp. 32–39.
16. **Wiggins-Camacho, J. D., Stevenson, K. J.** Indirect Electrochemical Degradation of Cyanide at Nitrogen-doped Carbon Nanotube Electrodes *Environmental Science and Technology* 45 2011: pp. 3650–3656.
17. **Valiūnienė, A., Baltrūnas, G., Keršulytė, V., Margarian, Ž., Valinčius, G.** The Degradation of Cyanide by Anodic Electrooxidation Using Different Anode Materials *Process Safety and Environmental Protection*  
<http://dx.doi.org/10.1016/j.psep.2012.06.007> (2012).
18. **Tamura, H., Aricado, A., Yoneyama, H., Matsuda, Y.** Anodic Oxidation of Potassium Cyanide on Platinum Electrode *Electrochimica Acta* 19 1974: pp. 273–277.
19. **Socrates, G.** Infrared and Raman Characteristic Group Frequencies: Tables and Charts. John Wiley & Sons Ltd. Chichester, 2004.
20. **Frantz, J. D.** Raman Spectra of Potassium Carbonate and Bicarbonate Aqueous Fluids at Elevated Temperatures and Pressures: Comparison with Theoretical Simulations *Chemical Geology* 152 1998: pp. 211–225.
21. **Popkirov, G.** An Experimental Approach to the Electrochemical Impedance Spectroscopy – Measurement Techniques and Data Validation *Current Topics in Electrochemistry* 7 2000: pp. 23–47.